

# A comparison of two structure-preserving integrators for nonlinear thermo-elastodynamics

M. Krüger, M. Groß, P. Betsch

*University of Siegen, Germany, {krueger, gross, betsch}@imr.mb.uni-siegen.de*

---

## Abstract

In this work, two different structure-preserving time integrators for coupled thermomechanical problems are compared. This comparison is done in the context of an adiabatic thermoelastic double pendulum. On the one hand a finite difference scheme is based on a Poissonian formulation of thermodynamics (GENERIC framework), on the other hand a hybrid (continuous/discontinuous) Galerkin method in time is formulated in the Lagrangian setting. The numerical example of a double pendulum shows that both time integrators possess an excellent longtime stability as well as an emersed robustness regarding large time step sizes. These advantageous properties are due to the algorithmic adherence to important physical characteristics of the problem.

## 1 Introduction

In the last two decades structure preserving time integrators, called energy-momentum consistent schemes, became more and more important. The main advantage of these integrators is the preservation of the underlying physical structure of the problem, which leads to a good longtime stability as well as an emersed robustness regarding large time step sizes.

A development of energy-momentum preserving time integrators for conservative problems is already done in Labudde & Greenspan [1, 2]. These works deal with the time integration of the motion of particles, and present a time integrator which uses Taylor series to define the values at the next time-step. The numerical time integration of nonlinear structural dynamics is adressed in Simo et al. [3–6]. Here, the energy-momentum schemes result from specific modifications of the midpoint rule applied to the Hamiltonian form of the equations of motion. An often used approach is the introduction of discrete derivatives, which goes back to Gonzalez [7, 8] and Gonzalez & Simo [9]. The authors describe nonlinear elastodynamics by using a Hamiltonian formulation. Hamiltonian dynamics can be regarded as special case of the Poisson formulation of dissipative dynamics. In Noels et al. [10], a structure-preserving time integrator originally developed for hyperelastic constitutive models is extended to finite hypoelasticity. Energy-momentum consistent time integrators for dissipative continuum dynamics are designed in Armero & Zambrana-Rojas [11], Groß & Betsch [12] and references therein. In these works, the conservation laws of momentum and the dissipative behaviour of the time evolution equations represent the physical structure which is maintained also in the discrete case. While the former work relies on the finite differences in time, the latter is based on Galerkin methods in time, Eriksson et al. [13], Cockburn [14] and Thomée [15], for instance. The **General Equations for Non-Equilibrium Reversible Irreversible Coupling** (see Öttinger [16]) yields a Poisson formulation of adiabatic thermodynamics. This GENERIC formalism is the starting point of the structure-preserving time integrator for discrete thermodynamics proposed recently by Romero [17].

In the present work four time integrators are compared. The well known midpoint rule and the hybrid Galerkin (hG) method are momentum preserving integrators. These integrators are the preliminary stage of the thermodynamically consistent (TC) integrator and the enhanced hybrid Galerkin (ehG) method, which are energy-momentum methods. The comparison will be done with regard to the temperature, the motion, the energy, the specific functional and the balances of both. The paper is structured as follows. At first, we describe the physical structure of the considered thermodynamic double pendulum. Then, we summarise the derivation of the TC integrator presented in Romero [17]. Subsequently, we derive a new energy-momentum consistent time integrator by carrying forward the procedure described in Groß & Betsch [12]. Both time integrators are then compared by means of numerical examples.

## 2 The thermoelastic double pendulum

We summarise the physical structure of the considered two-dimensional thermoelastic double pendulum in this section. Let  $q_1$  and  $q_2$  be the configuration vectors indicating the positions of the mass points  $m_1$  and  $m_2$ , respectively (see Figure 1). The vector  $r$  coincides with the difference vector  $q_2 - q_1$  between the two mass points.

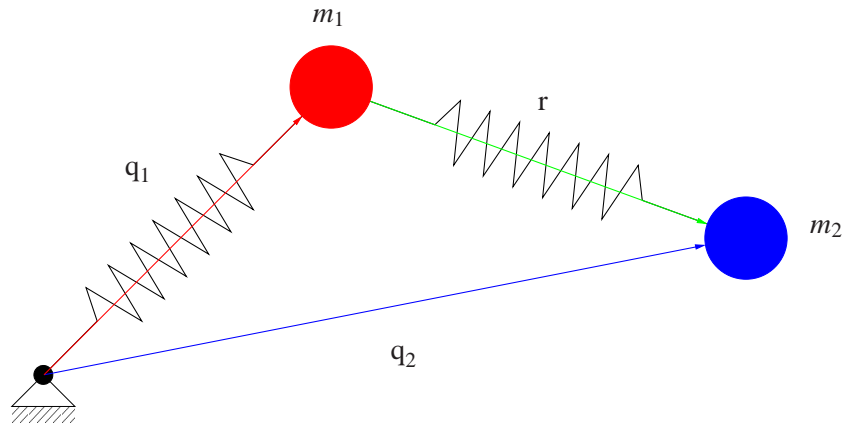


Figure 1: Thermoelastic double pendulum

The linear momentum vectors of the mass points are denoted by the vectors  $p_1$  and  $p_2$ , defined by

$$p_i = m_i v_i = m_i \dot{q}_i \quad (1)$$

where  $v_i$  denote the velocity vectors of the mass points. The linear momentum vectors are associated with the scalar products

$$\pi_i = p_i \cdot p_i \quad (2)$$

$i = 1, 2$ . The length of the springs in the reference configuration are denoted by  $\lambda_1^0$  and  $\lambda_2^0$ , respectively. The current length  $\lambda_1$  and  $\lambda_2$  are given by

$$\lambda_1 = \sqrt{c_1} = \sqrt{q_1 \cdot q_1} \quad \lambda_2 = \sqrt{c_2} = \sqrt{r \cdot r} \quad (3)$$

where  $c_i$  designate the scalar products of the direction vectors of the springs. The absolute temperatures in the springs are denoted by

$$\theta_i = \frac{\partial e_i}{\partial s_i} \quad (4)$$

and the relative temperatures  $\vartheta_i = \theta_i - \theta_\infty$  with respect to the reference temperature  $\theta_\infty$ ,  $i = 1, 2$ .

In the Hamiltonian way, the total energy of the double pendulum is defined as the functional

$$E(\boldsymbol{\pi}_1, \boldsymbol{\pi}_2, c_1, c_2, s_1, s_2) = T_1(\boldsymbol{\pi}_1) + T_2(\boldsymbol{\pi}_2) + e_1(c_1, s_1) + e_2(c_2, s_2) \quad (5)$$

decomposed in the kinetic energies  $T_i$  of the mass points and the internal energies  $e_i$  of the springs

$$T_i(\boldsymbol{\pi}_i) = \frac{1}{2m_i} \boldsymbol{\pi}_i \quad e_i(c_i, s_i) = \boldsymbol{\theta}_i s_i + \boldsymbol{\psi}_i(c_i, s_i) \quad (6)$$

Here,  $s_i$  and  $\boldsymbol{\psi}_i$  denote the entropies and the canonical free energies of the springs, respectively. The equations of motion for the double pendulum are then given by the Hamiltonian equations and the entropy evolution equations

$$\begin{aligned} \dot{q}_1 &= \frac{p_1}{m_1} & \dot{p}_1 &= -\frac{\partial(e_1 + e_2)}{\partial q_1} & \dot{s}_1 &= \kappa \left( \frac{\boldsymbol{\theta}_2}{\boldsymbol{\theta}_1} - 1 \right) \\ \dot{q}_2 &= \frac{p_2}{m_2} & \dot{p}_2 &= -\frac{\partial(e_1 + e_2)}{\partial q_2} & \dot{s}_2 &= \kappa \left( \frac{\boldsymbol{\theta}_1}{\boldsymbol{\theta}_2} - 1 \right) \end{aligned} \quad (7)$$

In the Lagrangian formulation, we refer to the functional

$$V(\boldsymbol{\pi}_1, \boldsymbol{\pi}_2, c_1, c_2, \boldsymbol{\theta}_1, \boldsymbol{\theta}_2) = T_1(\boldsymbol{\pi}_1) + T_2(\boldsymbol{\pi}_2) + \hat{e}_1(c_1, \boldsymbol{\theta}_1) + \hat{e}_2(c_2, \boldsymbol{\theta}_2) \quad (8)$$

as relative total energy based on the relative internal energy

$$\hat{e}_i(c_i, \boldsymbol{\theta}_i) = \boldsymbol{\vartheta}_i s_i(c_i, \boldsymbol{\theta}_i) + \hat{\boldsymbol{\psi}}_i(c_i, \boldsymbol{\theta}_i) \quad (9)$$

associated with the free energy  $\hat{\boldsymbol{\psi}} = \hat{\boldsymbol{\psi}}_a + \hat{\boldsymbol{\psi}}_b$  and the corresponding entropy  $S = s_a + s_b$ , which can be derived from the free energy by

$$s_i = -\frac{\partial \hat{\boldsymbol{\psi}}_i}{\partial \boldsymbol{\theta}_i} \quad (10)$$

The time rate of change of the free energies reads

$$\dot{\hat{\boldsymbol{\psi}}}_i = \frac{1}{2} S_i \dot{c}_i - s_i \dot{\boldsymbol{\theta}}_i \quad (11)$$

where  $S_i = 2 \frac{\partial \hat{\boldsymbol{\psi}}_i}{\partial c_i}$  characterises the stresses in the springs.

### 3 The TC integrator

In this section, we recall the TC integrator presented in Romero [17], which uses the GENERIC formalism (see Öttinger [16]), and enforces discrete directionality and degeneracy conditions in analogy to the continuous GENERIC formulation.

#### The GENERIC framework

The system under consideration is isolated. Looking at the time interval  $I = [t_0, T]$  of interest, we determine a function  $\mathbf{z}_t = \mathbf{z}(t) : I \rightarrow \mathcal{S}$  belonging to  $C^1(t_0, T)$  by solving the initial value problem

$$\begin{aligned} \dot{\mathbf{z}}_t &= \mathbf{L}(\mathbf{z}_t) \nabla E(\mathbf{z}_t) + \mathbf{M}(\mathbf{z}_t) \nabla S(\mathbf{z}_t) \\ \mathbf{z}(t_0) &= \mathbf{z}_0 \end{aligned} \quad (12)$$

where  $\mathbf{z}_0$  is the initial state vector. The matrix  $\mathbf{L}$  and the matrix  $\mathbf{M}$  denote the Poisson matrix and the friction matrix, respectively. The gradient  $\nabla$  reflects the derivative with respect to the state vector

$$\mathbf{z} = [q_1, q_2, p_1, p_2, s_1, s_2] \quad (13)$$

The matrix  $L$  (skew-symmetric) represents the reversible part and the matrix  $M$  (symmetric, positive semidefinite) characterises the irreversible part. In addition to that we have the degeneracy conditions

$$L(z_t) \nabla S(z_t) = M(z_t) \nabla E(z_t) = 0 \quad (14)$$

which lead to two consequences

$$\dot{E}(z_t) = 0 \quad \dot{S}(z_t) \geq 0 \quad (15)$$

Considering the Lyapunov-function  $L = E - \theta_\infty S$  the initial value problem (12) fulfils the stability estimate

$$\dot{L} = -D^{cd u} \leq 0 \quad (16)$$

where  $D^{cd u}$  indicates the non-negative total dissipation arising from the heat transfer.

### The time stepping scheme

The interval  $I$  has to be divided into subintervals  $I_n = [t_n, t_{n+1}]$  with the lengths  $h_n = t_{n+1} - t_n$ . Each time point  $t_n$  leads then to a state variable  $z_n$ . The TC integrator has the form

$$\frac{z_{n+1} - z_n}{h_n} = \mathcal{L}(z_{n+1}, z_n) \mathcal{D}E(z_{n+1}, z_n) + \mathcal{M}(z_{n+1}, z_n) \mathcal{D}S(z_{n+1}, z_n) \quad (17)$$

where the discrete operators  $\mathcal{L}$  and  $\mathcal{M}$ , and  $\mathcal{D}E$  and  $\mathcal{D}S$  denote discrete gradients. Since the Eqs. (14) and (15) must also hold for the discrete counterparts, we get the degeneracy conditions

$$\mathcal{L}(z_n, z_{n+1}) \mathcal{D}S(z_n, z_{n+1}) = \mathcal{M}(z_n, z_{n+1}) \mathcal{D}E(z_n, z_{n+1}) = 0 \quad (18)$$

and the directionality conditions

$$\begin{aligned} \mathcal{D}E(z_n, z_{n+1})(z_{n+1} - z_n) &= E(z_{n+1}) - E(z_n) \\ \mathcal{D}S(z_n, z_{n+1})(z_{n+1} - z_n) &= S(z_{n+1}) - S(z_n) \end{aligned} \quad (19)$$

in the discrete setting. In Romero [17] is shown, that the TC integrator fulfils these conditions, such that the total energy  $E$  is conserved and the entropy  $S$  never decreases. According to a theorem of Emmy Noether additional balance laws are fulfilled if these functions are defined by

$$\begin{aligned} E(z) &= \tilde{E}(\pi(z)) = \frac{\pi_1}{2m_1} + \frac{\pi_2}{2m_2} + e_a(c_1, s_1) + e_2(c_2, s_2) \\ S(z) &= \tilde{S}(\pi(z)) = s_1 + s_2 \end{aligned} \quad (20)$$

via the vector

$$\pi = [c_1 \quad c_2 \quad \pi_1 \quad \pi_2 \quad s_1 \quad s_2 \quad q_1 \cdot p_1 \quad q_2 \cdot p_2 \quad q_1 \cdot q_2]^T \quad (21)$$

of invariants. In order to satisfy these balance laws as well, the discrete gradients are evaluated by the chain rule of differentiation. Eq. (17) can now be written as

$$\frac{z_{n+1} - z_n}{h_n} = \mathcal{L} \nabla \pi(z_{n+\frac{1}{2}})^T \mathcal{D}\tilde{E}(\pi(z_{n+1}), \pi(z_n)) + \mathcal{M} \nabla \pi(z_{n+\frac{1}{2}})^T \mathcal{D}\tilde{S}(\pi(z_{n+1}), \pi(z_n)) \quad (22)$$

with the discrete matrices  $\mathcal{L}$  and  $\mathcal{M}$ . These matrices are given by

$$\mathcal{L} = L \quad \mathcal{M} = \begin{bmatrix} 0^{8 \times 8} & 0^{8 \times 1} & 0^{8 \times 1} \\ 0^{1 \times 8} & \kappa \frac{\theta_1^*}{\theta_1^*} & -\kappa \\ 0^{1 \times 8} & -\kappa & \kappa \frac{\theta_1^*}{\theta_2^*} \end{bmatrix} \quad (23)$$

with

$$\theta_1^* = \mathcal{D}_{s_1} e_1 \quad \theta_2^* = \mathcal{D}_{s_2} e_2 \quad (24)$$

Carefully accounting for the argument  $(z_n, z_{n+1})$ , the directionality conditions are guaranteed by partitioned discrete gradients (Gonzalez [7]). Recall, if  $c_{i_n} = c_{i_{n+1}}$  and  $s_{i_n} = s_{i_{n+1}}$ , we obtain the midpoint rule according to L'Hopital's rule. Employing Eq. (23) into Eq. (22), we get the discrete time evolution equations

$$\begin{aligned}
\frac{q_{1_{n+1}} - q_{1_n}}{h_n} &= \frac{1}{m_1} p_{1_{n+\frac{1}{2}}} \\
\frac{q_{2_{n+1}} - q_{2_n}}{h_n} &= \frac{1}{m_2} p_{2_{n+\frac{1}{2}}} \\
\frac{p_{1_{n+1}} - p_{1_n}}{h_n} &= -2 \mathcal{D}_{c_1} e_1 q_{1_{n+\frac{1}{2}}} + 2 \mathcal{D}_{c_2} e_2 r_{n+\frac{1}{2}} \\
\frac{p_{2_{n+1}} - p_{2_n}}{h_n} &= -2 \mathcal{D}_{c_2} e_2 r_{n+\frac{1}{2}} \\
\frac{s_{1_{n+1}} - s_{1_n}}{h_n} &= \kappa \left( \frac{\theta_2^*}{\theta_1^*} - 1 \right) \\
\frac{s_{2_{n+1}} - s_{2_n}}{h_n} &= \kappa \left( \frac{\theta_1^*}{\theta_2^*} - 1 \right)
\end{aligned} \tag{25}$$

which fulfil the stability estimate  $L(z_{n+1}) \leq L(z_n)$  on each time step, analogously to the continuous time evolution equations.

## 4 The enhanced hybrid Galerkin method

The second structure-preserving integrator is developed in Groß & Betsch [12] for general continuum thermo-elastodynamics. This scheme emanates from a new hybrid (continuous/discontinuous) Galerkin method in time and can be regarded as extension of the previously developed energy momentum (EM) schemes of Betsch & Steinmann [18] and Groß et al. [19] to coupled thermoelastic problems. In the case of the thermoelastic double pendulum the underlying Lagrangian description relies on the state vector

$$z = [q_1, q_2, v_1, v_2, \theta_1, \theta_2] \tag{26}$$

We rewrite the equations of motion of Eq. (7), and obtain

$$\begin{aligned}
\dot{q}_1 &= v_1 \\
\dot{q}_2 &= v_2 \\
\dot{p}_1 &= S_2 r - S_1 q_1 \\
\dot{p}_2 &= -S_2 r
\end{aligned} \tag{27}$$

The stability estimate is derived from the Lyapunov-function  $V(\pi_1, \pi_2, c_1, c_2, \theta_1, \theta_2)$  defined in Eq. (8) and leads after applying the fundamental theorem of calculus to the difference

$$V_{t=T} - V_{t=t_0} = - \int_I D^{cd} u \leq 0 \tag{28}$$

on the time interval  $I$  of interest.

### The weak forms

The weak forms can be deduced from the strong forms by multiplication with test functions and integration over time. These test functions have to lead to a system of equations which fulfil among the initial conditions also the stability estimate in Eq. (28).

At first, we derive the weak equations of motion by looking at the kinetic energies  $T_i$ ,  $i = 1, 2$ . The

fundamental theorem of calculus leads to the two following forms, after using the equations of motion (27)<sub>1-4</sub>

$$\begin{aligned} \int_I \delta \dot{\mathbf{p}}_i \cdot \mathbf{v}_i &= \int_I \delta \dot{\mathbf{p}}_i \cdot \dot{\mathbf{q}}_i \\ \int_I \dot{\mathbf{p}}_i \cdot \delta \dot{\mathbf{q}}_i &= - \int_I \frac{\partial \hat{\Psi}}{\partial \mathbf{q}_i} \cdot \delta \dot{\mathbf{q}}_i \end{aligned} \quad (29)$$

The realisation of the non-negative Dissipation  $D^{cd\mu}$  is only guaranteed with the test functions  $\vartheta_i$  in the weak form. This test functions must have the same polynomial degree as the trial function  $\theta_i$ . In the end, a dG-Method with an energy consistent jump term is necessary and yield the form

$$\frac{[[\hat{e}_i(t_0)]]}{\vartheta_{i,t=t_0}^+} \delta \theta_{i,t=t_0}^+ + \int_I \dot{s}_i \delta \theta_i = \int_I \kappa \left( \frac{\theta_j}{\theta_i} - 1 \right) \delta \theta_i \quad j \neq i \in \{1, 2\} \quad (30)$$

These weak forms lead to a discontinuous approximation of the temperatures at time  $t_0$ .

### Time finite element approximation

We divide the time interval  $I = [t_0, T]$  into  $m$  subintervals  $I_n = [t_n, t_{n+1}]$  with  $n \in M = 1, 2, \dots, m$  for the finite element approximation in time. The time step size  $h_n$  is given by the difference  $t_{n+1} - t_n$  with the linear mapping

$$t(\alpha) = (1 - \alpha)t_n + \alpha t_{n+1} \quad (31)$$

of an unit interval  $I_\alpha = [0, 1]$  to the interval  $I_n$  with  $\alpha \in I_\alpha$ . A piecewise continuous or discontinuous time evolution  $[\cdot](t)$ , respectively, is then defined by the linear operators

$$[\cdot]_{n+\alpha} = (1 - \alpha)[\cdot]_n + \alpha[\cdot]_{n+1} \quad [\cdot]_{n+\alpha}^+ = (1 - \alpha)[\cdot]_n^+ + \alpha[\cdot]_{n+1}^+ \quad (32)$$

with their derivatives  $[\cdot]_{n+\alpha}^\circ$  and  $[\cdot]_{n+\alpha}^{\circ+}$  with respect to  $\alpha$ . We obtain a Petrov-Galerkin approximation with the test function  $\delta[\cdot]_{n+\alpha} = \delta[\cdot]_n$  for the equations of motion. For the entropy evolution equations, the test functions are the same as the trial functions, which means the Bubnov-Galerkin approximation  $\delta[\cdot]_{n+\alpha}^+ = (1 - \alpha)\delta[\cdot]_n^+ + \alpha\delta[\cdot]_{n+1}^+$ . The stability estimate has now to hold on each subinterval  $I_n$ , such that

$$V_{n+1} - V_n + h_n \int_{I_\alpha} D^{cd\mu} = 0 \quad (33)$$

Therefore, the division into subintervals and the transformation to the time interval  $I_\alpha$  leads to the following approximation of the weak forms

$$\begin{aligned} \delta \dot{\mathbf{p}}_{i_n} \cdot \mathbf{v}_{i_{n+\frac{1}{2}}} &= \frac{1}{h_n} \delta \dot{\mathbf{p}}_{i_n} \cdot (\mathbf{q}_{i_{n+1}} - \mathbf{q}_{i_n}) \\ \frac{1}{h_n} (\mathbf{p}_{i_{n+1}} - \mathbf{p}_{i_n}) \cdot \delta \dot{\mathbf{q}}_{i_n} &= - \left( \frac{\partial \hat{\Psi}}{\partial \mathbf{q}_i} \right)_{\frac{1}{2}} \cdot \delta \dot{\mathbf{q}}_{i_n} \\ \frac{\hat{e}_{i_n}^+ - \hat{e}_{i_n}}{\theta_{i_n}^+ - \theta_{i_n}} \delta \theta_{i_n}^+ + (s_{i_{n+1}} - s_{i_n}^+) \delta \theta_{i_{n+\frac{1}{2}}}^+ &= \frac{h_n}{2} \sum_{l=1}^2 \kappa \left( \frac{\theta_{j_{n+\xi_l}}^+}{\theta_{i_{n+\xi_l}}^+} - 1 \right) \delta \theta_{i_{n+\xi_l}}^+ \end{aligned} \quad (34)$$

For a numerical exact integration of the first weak equations of motion, one Gaussian quadrature point  $\xi_1 = \frac{1}{2}$  and a weight  $w_1 = 1$  (the midpoint rule) is necessary. The finite element approximation is also applied for the second weak equations of motion. Note that this leads to total angular momentum conservation. We have to apply a two-point Gaussian quadrature rule for calculating the integrals of the entropy evolution equation with their piecewise linear testfunctions, in contrast to the equations of motion with their piecewise constant test functions. This two Gauss points are given by  $\xi_1 = \frac{1-\sqrt{3}}{2}$  and  $\xi_2 = 1 - \xi_1$  with their corresponding weights  $w_1 = w_2 = \frac{1}{2}$ . The integral on the left side is already numerically exact calculated by using the midpoint rule. In contrast to that, the integral on the right side is generally not integrated exactly. The hG method would then be given by the evaluation of the  $c_i$  at the midpoint  $c_{1\frac{1}{2}} = \mathbf{q}_{1_{n+\frac{1}{2}}} \mathbf{q}_{1_{n+\frac{1}{2}}}$  and  $c_{2\frac{1}{2}} = \mathbf{r}_{n+\frac{1}{2}} \mathbf{r}_{n+\frac{1}{2}}$  and  $\theta_{i_{n+\xi_l}}^+ = (1 - \xi_l) \theta_{i_n}^+ + \xi_l \theta_{i_{n+1}}^+$ .

## Stress approximation

The satisfaction of the angular momentum balance and the stability estimate in the discrete setting is done with a new stress approximation

$$\bar{S}_{i\frac{1}{2}} = S_{i\frac{1}{2}} + \hat{S}_{i\frac{1}{2}} \quad (35)$$

instead of the ordinary approximation  $S_{i\frac{1}{2}}$ . Furthermore, we use the approximation  $\bar{c}_{i\frac{1}{2}} = c_{i_{n+\frac{1}{2}}}$  for the  $c_i$ . The derivation of the algorithmic stress  $\hat{S}_{i\frac{1}{2}}$  begins with the formulation of the constraint

$$G_i(\hat{S}_{i\frac{1}{2}}) = \hat{e}_{i_{n+1}} - \hat{e}_{i_n}^+ - \hat{e}_{i_{n+\frac{1}{2}}} - \frac{1}{2} \hat{S}_{i\frac{1}{2}} (c_{i_{n+1}} - c_{i_n}) \quad (36)$$

Then, we minimise the functional

$$F_i(\hat{S}_{i\frac{1}{2}}, \mu_i) = \mu_i G_i(\hat{S}_{i\frac{1}{2}}) + \frac{1}{2} \hat{S}_{i\frac{1}{2}}^2 \quad (37)$$

where  $\mu_i$  denotes a Lagrange multiplier corresponding to the constraint. The total stress approximation  $\bar{S}_{i\frac{1}{2}}$  then reads

$$\bar{S}_{i\frac{1}{2}} = 2 \frac{\hat{e}_{i_{n+1}} - \hat{e}_{i_n}^+ - [s_{i_{n+1}} - s_{i_n}^+] \vartheta_{i_{n+\frac{1}{2}}}^+}{c_{i_{n+1}} - c_{i_n}} \quad (38)$$

In the special case of  $c_{i_{n+1}} = c_{i_n}$  the total stress approximation is equivalent to the ordinary approximation  $\bar{S}_{i\frac{1}{2}} = S_{i\frac{1}{2}}$ . This total stress approximation leads to the following discrete equations for the thermoelastic double pendulum:

$$\begin{aligned} \frac{q_{1_{n+1}} - q_{1_n}}{h_n} &= v_{1_{n+\frac{1}{2}}} \\ \frac{q_{2_{n+1}} - q_{2_n}}{h_n} &= v_{2_{n+\frac{1}{2}}} \\ \frac{p_{1_{n+1}} - p_{1_n}}{h_n} &= -\bar{S}_{1\frac{1}{2}} q_{1_{n+\frac{1}{2}}} + \bar{S}_{2\frac{1}{2}} r_{n+\frac{1}{2}} \\ \frac{p_{2_{n+1}} - p_{2_n}}{h_n} &= -\bar{S}_{2\frac{1}{2}} r_{n+\frac{1}{2}} \end{aligned} \quad (39)$$

$$\begin{aligned} \left[ \begin{array}{c} \frac{\hat{e}_{1_n}^+ - \hat{e}_{1_n}}{\theta_{1_n}^+ - \theta_\infty} + \frac{1}{2} (s_{1_{n+1}} - s_{1_n}^+) \\ \frac{1}{2} (s_{1_{n+1}} - s_{1_n}^+) \end{array} \right] - h_n \frac{\kappa}{2} \sum_{l=1}^2 \begin{bmatrix} 1 - \xi_l \\ \xi_l \end{bmatrix} \left( \frac{\theta_{2_{n+\xi_l}}^+}{\theta_{1_{n+\xi_l}}^+} - 1 \right) &= 0 \\ \left[ \begin{array}{c} \frac{\hat{e}_{2_n}^+ - \hat{e}_{2_n}}{\theta_{2_n}^+ - \theta_\infty} + \frac{1}{2} (s_{2_{n+1}} - s_{2_n}^+) \\ \frac{1}{2} (s_{2_{n+1}} - s_{2_n}^+) \end{array} \right] - h_n \frac{\kappa}{2} \sum_{l=1}^2 \begin{bmatrix} 1 - \xi_l \\ \xi_l \end{bmatrix} \left( \frac{\theta_{1_{n+\xi_l}}^+}{\theta_{2_{n+\xi_l}}^+} - 1 \right) &= 0 \end{aligned} \quad (40)$$

## 5 The numerical example

We consider the motion of an adiabatic thermoelastic double pendulum initiated by the initial positions  $q_i^0$  [m], the initial linear momenta  $p_i^0$  [N s] as well as the initial temperatures  $\theta_i^0$  [K], given by

$$\begin{aligned} q_1^0 &= \begin{bmatrix} 1 \\ 0 \end{bmatrix} & p_1^0 &= \begin{bmatrix} 0 \\ 1 \end{bmatrix} & \theta_1^0 &= 380 \\ q_2^0 &= \begin{bmatrix} 2, 2 \\ 0 \end{bmatrix} & p_2^0 &= \begin{bmatrix} 0 \\ 4, 4 \end{bmatrix} & \theta_2^0 &= 310 \end{aligned} \quad (41)$$

In the numerical examples, we choose a free energy  $\hat{\psi}_i$  introduced in Romero [17], which is given by

$$\hat{\psi}_i = \frac{K_i}{2} \log^2 \left( \frac{\lambda_i}{\lambda_i^0} \right) - \beta_i \vartheta_i \log \left( \frac{\lambda_i}{\lambda_i^0} \right) + k_i \left[ \vartheta_i - \theta_i \log \left( \frac{\theta_i}{\theta_\infty} \right) \right] \quad (42)$$

Further, the mass points  $m_i$  [kg], the reference length of the considered elastomer springs  $\lambda_i^0$  [m] and the stiffness parameters  $K_i$  [J] read

$$m_1 = 1 \quad m_2 = 2 \quad \lambda_1^0 = 2 \quad \lambda_2^0 = 1 \quad K_1 = K_2 = 10000 \quad (43)$$

The reference temperature  $\theta_\infty$  [K], the conductivity constant  $\kappa$  [W/K], the heat capacity  $k_i$  [J/K] and the coupling parameter  $\beta_i$  [J/K] are given by

$$\theta_\infty = 300 \quad \kappa = 10 \quad k_i = 1000 \quad \beta_i = 0,2 \quad i \in [1,2] \quad (44)$$

The considered time interval of interest is  $I = [0, 50]$ s for the quasi-stiff motion of the double pendulum. The system is solved with the Newton-Raphson method with the tolerance  $\varepsilon = 10^{-8}$  [J].

### The reference solution (close time-mesh)

At first we take a look at the reference solutions for the stiff system, which is done with the TC algorithm. The reference solution for the stiff system is given by a time step size  $\Delta t = 0.0001$ s. In Figure 2 are shown the temperatures  $\theta_1$  and  $\theta_2$ , the length of the vector  $q_1$ , the energy  $E$  and the functional  $L$ . The length of the coordinate vector  $q_1$ , which reflects the length of the first spring, oscillates in the range  $[1, 4]$ . It is obvious that the energy  $E$  rests on a constant level and that the Lyapunov-function  $L$  is always decreasing.

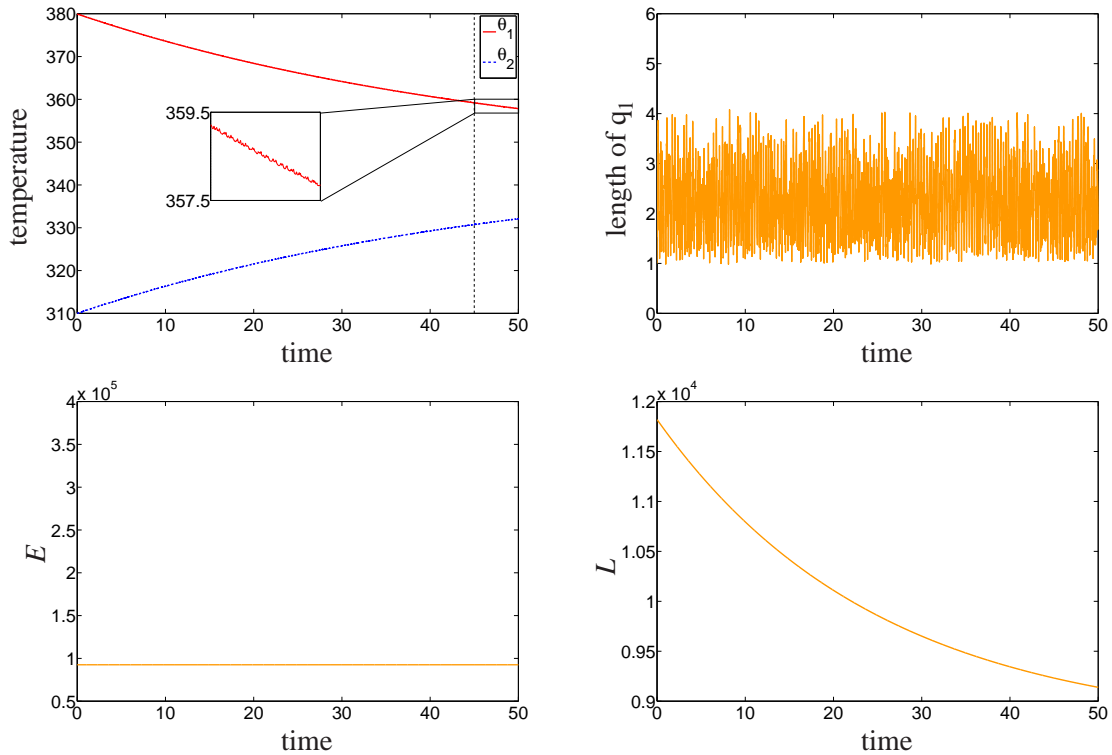


Figure 2: Reference solution with the TC integrator for a time step size  $\Delta t = 0.0001$

### Coarse time-mesh

We start the comparison of the four methods with the temperatures  $\theta_1$  and  $\theta_2$  and the length of the coordinate vector  $q_1$  in the Figure 3 at a time step size  $\Delta t = 0.015$ s. Comparing the midpoint rule and the hG method with the reference solution, we can see that the temperature more oscillates as the TC

algorithm, the ehG method and the reference solution, which are nearly the same (compare Figure 2). Once more the length of the coordinate  $q_1$  explodes after a few seconds to the multiple of its reference length. This leads to completely wrong results for the standard methods.

The total energy  $E$ , the Lyapunov-functions  $L$  and  $V$  are shown in Figure 4. The TC algorithm and the ehG method lead to the same constant value for the energy  $E$  as the reference solution. The Lyapunov-function  $L$  of the TC algorithm and the Lyapunov-function  $V$  of the ehG method yield the decreasing behaviour which is known of Figure 2. Both functionals amount to the same results. This behaviour of the energy  $E$  and the Lyapunov-functions  $L$  and  $V$  are fulfilled for the four different time step sizes  $\Delta t = [0.006 \ 0.009 \ 0.012 \ 0.015]$ s. In contrast to that the midpoint rule as well as the hG method result in a blow-up for large time step sizes. The larger the time step size, the earlier the energy blows up. This is also valid for the decreasing behaviour of the functional, which cannot be fulfilled for large time step sizes by the standard methods (midpoint rule, hG method). The energy growth lays in the range of 100 – 300%. This energy growth tends to a wrong behaviour of the Lyapunov-functions  $L$  and  $V$ . The TC algorithm and the ehG method show the same results as the reference solution (compare Figure 2).

A closer look to the energy  $E$  and the Lyapunov-functions  $L$  and  $V$  is given by the  $\Delta E$ -function and the balance of the Lyapunov-functions. These both have to be fulfilled for the underlying tolerance  $\varepsilon$  of the Newton-Raphson iteration. The results of the hG method are comparable with that of the midpoint rule. As we can see in Figure 5, the midpoint rule and the hG method can not fulfil these conditions, because the integration is not exact. Using now the TC algorithm the absolute value of the  $\Delta E$ -function and the balance of the Lyapunov-functional  $L$  is below the tolerance  $\varepsilon$  (see Figure 5). The ehG method does not fulfil the conservation of the total energy  $E$  numerically exactly, because the method enforces the discrete fundamental theorem of calculus

$$\hat{e}_{i_{n+1}} - \hat{e}_{i_n} = \hat{e}_{i_{n+\frac{1}{2}}} \quad (45)$$

in order to satisfy the stability estimate in Eq. (28) as a physical structure equation which is not restricted to adiabatic systems (see Groß & Betsch [12]). The TC algorithm enforces the discrete fundamental theorem of calculus

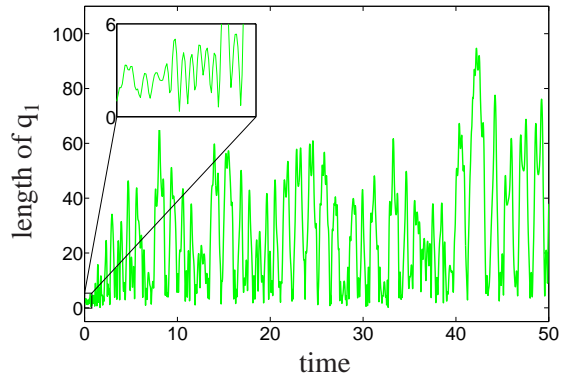
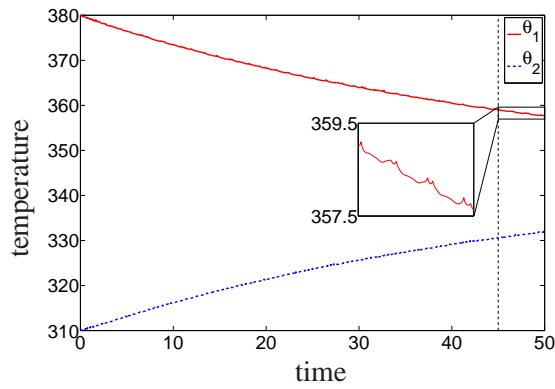
$$e_{i_{n+1}} - e_{i_n} = \dot{e}_{i_{n+\frac{1}{2}}} \quad (46)$$

with respect to the functions  $e_i$  by enforcing the degeneracy conditions in Eq. (18). This is possible for this adiabatic thermodynamic system.

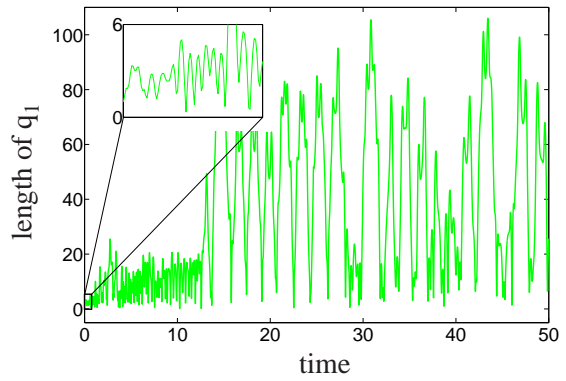
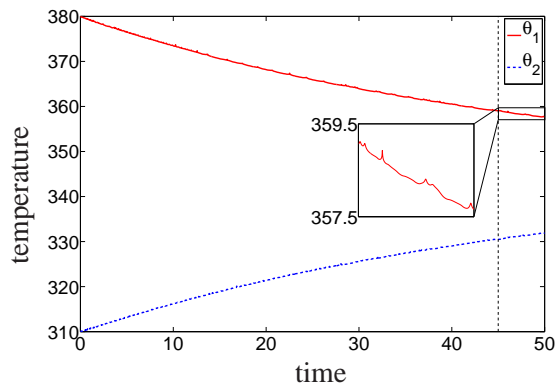
## 6 Summary

Structure-preserving time integrators are of great interest. The advantage of these time integrators is the preservation of the physical structure equations of the underlying problem. This leads to an excellent longtime stability as well as an emersed robustness regarding large time step sizes. In this work, we compare two different structure-preserving time integrators for an adiabatic thermoelastic double pendulum. The first, the so-called TC algorithm, is a finite difference scheme restricted to second-order accuracy, which is based on a Poissonian formulation of thermodynamics (GENERIC framework). The second, the ehG method, is a hybrid (continuous/discontinuous) Galerkin method in time formulated in the Lagrangian point of view and appropriate for higher-order accuracy. Both integrators possess comparable numerical stability and robustness, but possess a distinction in the preserved physical structure. The TC algorithm exploit the fact that the double pendulum represents an adiabatic system, and leads to an exactly conserved total energy. The ehG method preserves as physical structure equation a stability estimate based on the relative total energy, which is not restricted to adiabatic systems. Numerical examples uniquely reveal that both methods exhibit the mentioned advantages of structure-preserving time integrators.

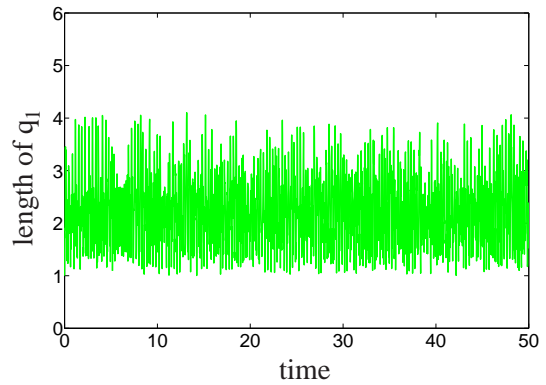
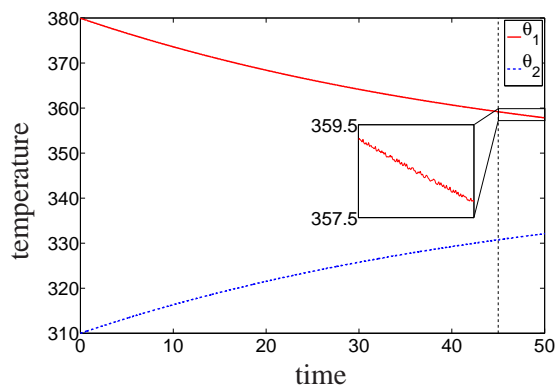
midpoint rule  $\Delta t = 0.015s$



hG method  $\Delta t = 0.015s$



TC algorithm  $\Delta t = 0.015s$



ehG method  $\Delta t = 0.015s$

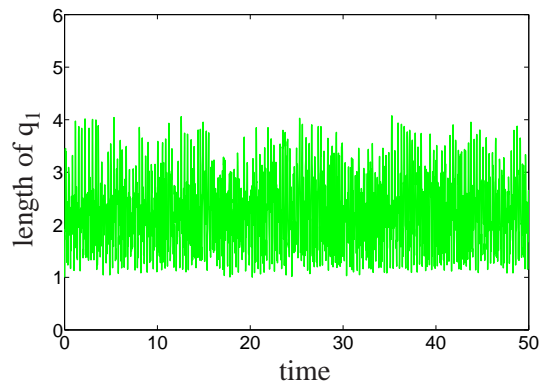
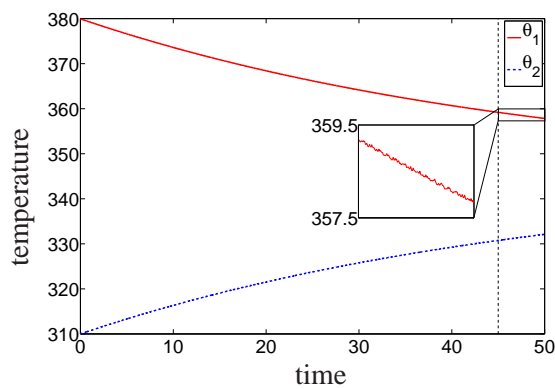
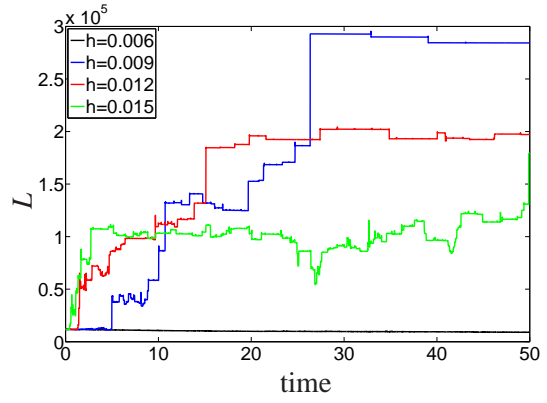
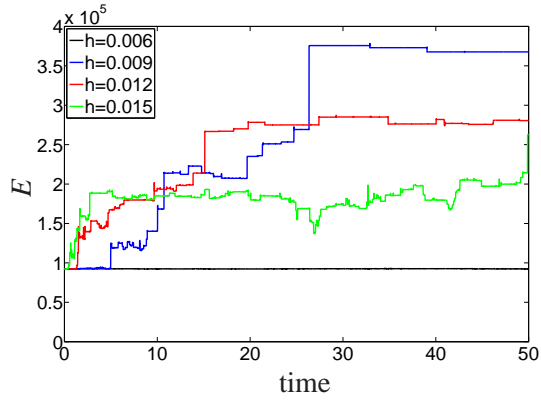
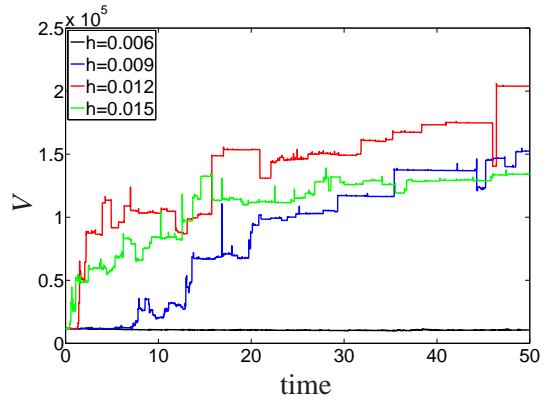
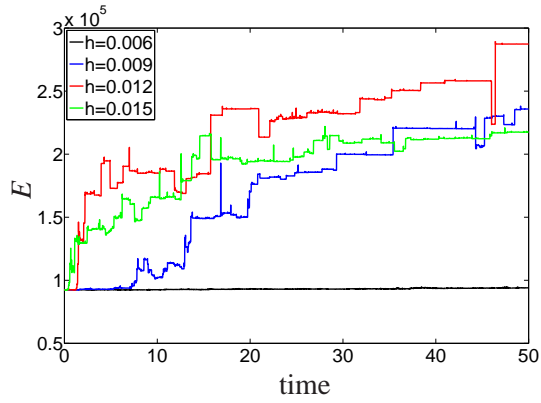


Figure 3: Stiff system - temperatures  $\theta_1$ ,  $\theta_2$  and the length of  $q_1$  of the four methods for the time step size  $\Delta t = 0.015$

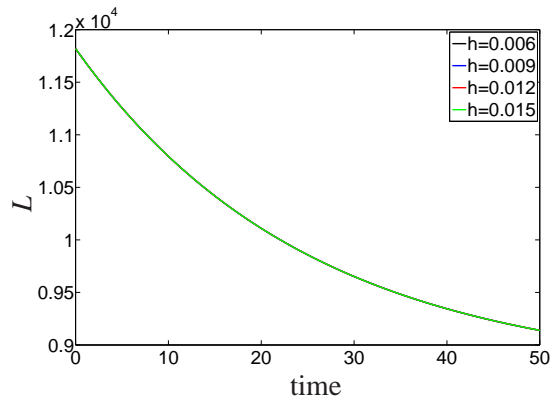
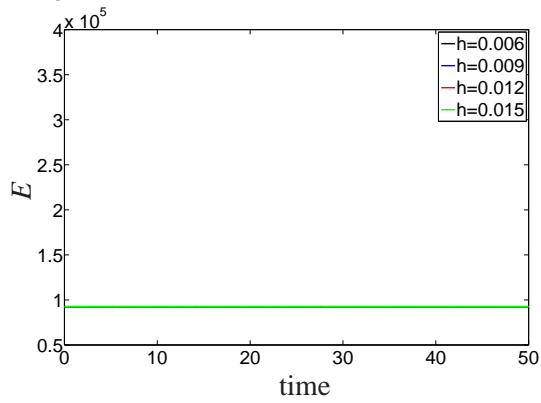
midpoint rule



hG method



TC algorithm



ehG method

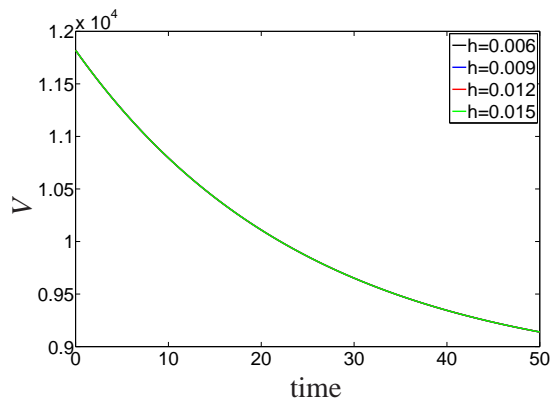
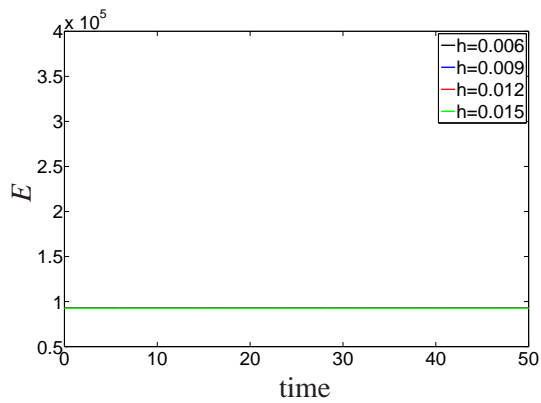
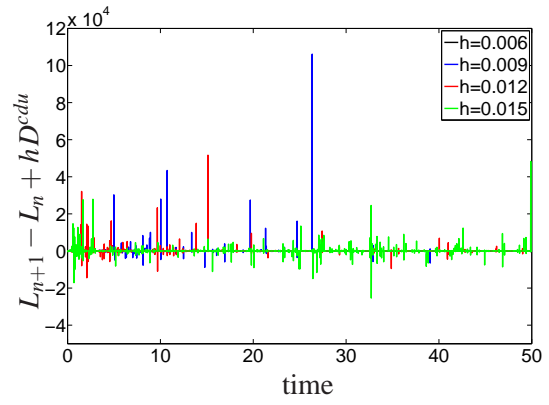
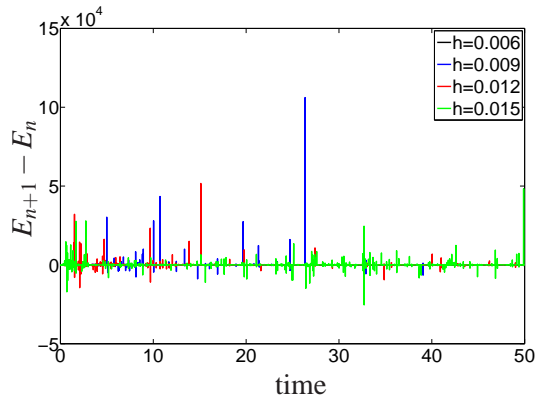
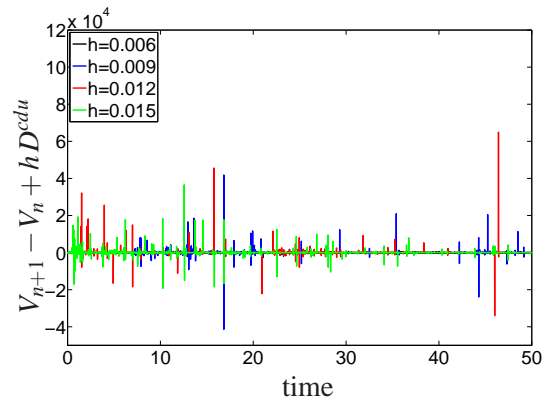
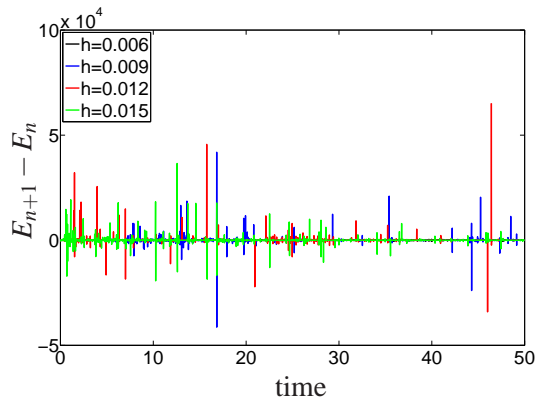


Figure 4: Stiff system - energy  $E$  and the Lyapunov-functions  $L$  and  $V$  of the four methods for different time step sizes

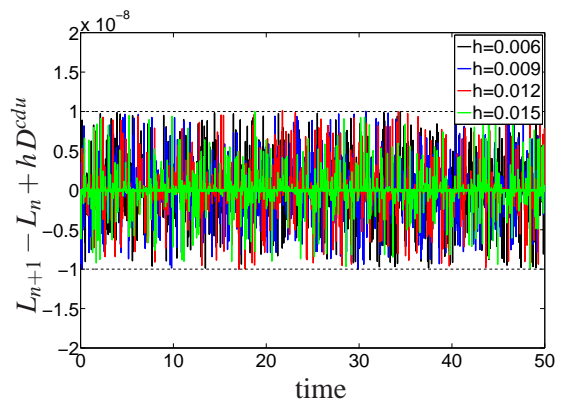
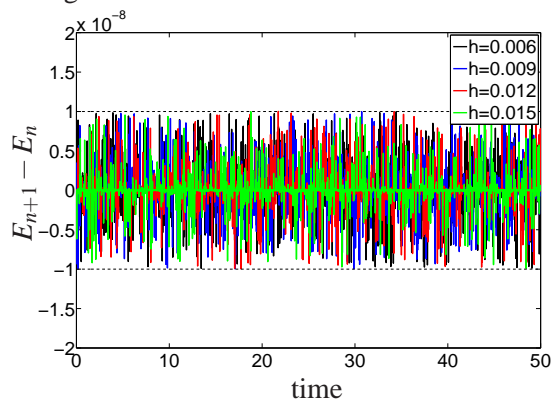
midpoint rule



hG method



TC algorithm



ehG method

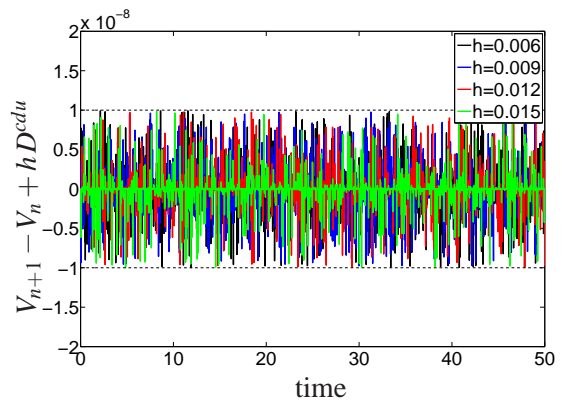
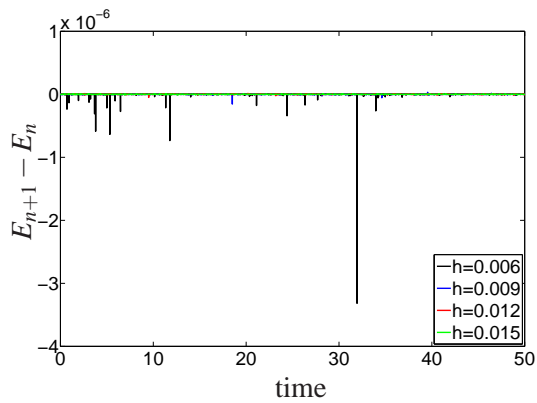


Figure 5: Stiff system -  $\Delta E$  and the balances of the Lyapunov-functions  $L$  and  $V$  of the four methods for different time step sizes

## References

- [1] R.A. Labudde and D. Greenspan. Energy and momentum conserving methods of arbitrary order for the numerical integration of equations of motion - i. Motion of a single particle. *Numerische Mathematik*, 25:323–346, 1976.
- [2] R.A. Labudde and D. Greenspan. Energy and momentum conserving methods of arbitrary order for the numerical integration of equations of motion - i. Motion of a system of particles. *Numerische Mathematik*, 26:1–16, 1976.
- [3] J.C. Simo, N. Tarnow, and K. K. Wong. Exact energy-momentum conserving algorithms and symplectic schemes for nonlinear dynamics. *Computer Methods in Applied Mechanics and Engineering*, 100(1):63–116, 1992.
- [4] J.C. Simo and N. Tarnow. The discrete energy-momentum method. Conserving algorithms for nonlinear elastodynamics. *Journal of Applied Mathematics and Physics*, 43:757–792, 1992.
- [5] J.C. Simo and N. Tarnow. A new energy and momentum conserving algorithm for the non-linear dynamics of shells. *International Journal for Numerical Methods in Engineering*, 37:2527–2549, 1994.
- [6] J.C. Simo, N. Tarnow, and M. Doblare. Non-linear dynamics of three-dimensional rods: Exakt energy and momentum conserving algorithms. *International Journal for Numerical Methods in Engineering*, 38:1431–1473, 1995.
- [7] O. Gonzalez. *Design and analysis of conserving integrators for nonlinear Hamiltonian systems with symmetry*. Ph.D. Thesis, Department of Mechanical Engineering, Stanford University, 1996.
- [8] O. Gonzalez. Time integration and discrete hamiltonian systems. *Journal of Nonlinear science*, 132:165–174, 1996.
- [9] O. Gonzalez and J.C. Simo. Exact Energy and Momentum Conserving Algorithms for General Models in Nonlinear Elasticity. *Computer Methods in Applied Mechanics and Engineering*, 190:1763–1783, 2000.
- [10] L. Noels, L. Stainier, and J.P. Ponthot. An energy-momentum conserving algorithm for nonlinear hypoelastic constitutive models. *Computer Methods in Applied Mechanics and Engineering*, 59:83–114, 2004.
- [11] F. Armero and C. Zambrana-Rojas. Volume preserving energy-momentum schemes for isochoric multiplicative plasticity. *Computer Methods in Applied Mechanics and Engineering*, 196(41-44):4130–4159, 2007.
- [12] M. Groß and P. Betsch. Galerkin-based energy-momentum consistent time integrators for classical nonlinear thermoelastodynamics. submitted for publication.
- [13] K. Eriksson, D. Estep, P. Hansbo, and C. Johnson. *Computational differential equations*. Cambridge University Press, 1996.
- [14] B. Cockburn. Discontinuous Galerkin Methods. *Z. Angew. Math. Meth.*, 11:731–754, 2003.
- [15] V. Thomée. *Galerkin finite methods for parabolic problems*. Springer, 1997.
- [16] H.C. Öttinger. *Beyond equilibrium thermodynamics*. Wiley, 2005.
- [17] I. Romero. Thermodynamically consistent time-stepping algorithms for non-linear thermomechanical systems. *International Journal for Numerical Methods in Engineering*, 79:706–732, 2009.
- [18] P. Betsch and P. Steinmann. Conservation properties of a time FE method-Part II: Time stepping schemes for non-linear elastodynamics. *International Journal for Numerical Methods in Engineering*, 50:1931–1955, 2001.
- [19] M. Groß, P. Betsch, and P. Steinmann. Conservation properties of a time FE method-Part IV: Higher order energy and momentum conserving schemes. *International Journal for Numerical Methods in Engineering*, 63:1849–1897, 2005.